Low-Molecular-Weight Protein Tyrosine Phosphatases of *Bacillus subtilis*†

Lucia Musumeci,[1] Cristina Bongiorni,[2] Lutz Tautz,[1] Robert A. Edwards,[1,3]
Andrei Osterman,[1] Marta Perego,[2] Tomas Mustelin,[1] and Nunzio Bottini[1]*

*Inflammatory and Infectious Diseases Center, The Burnham Institute, 10901 North Torrey Pines Road,
La Jolla, California 92037[1]; Division of Cellular Biology, Department of Molecular and Experimental
Medicine, The Scripps Research Institute, 10550 North Torrey Pines Road, La Jolla,
California 92037[2]; and Fellowship for the Interpretation of Genomes, Center for
Microbial Sciences, San Diego State University, San Diego, California 92182[3]*

In gram-negative organisms, enzymes belonging to the low-molecular-weight protein tyrosine phosphatase (LMPTP) family are involved in the regulation of important physiological functions, including stress resistance and synthesis of the polysaccharide capsule. LMPTPs have been identified also in gram-positive bacteria, but their functions in these organisms are presently unknown. We cloned two putative LMPTPs from *Bacillus subtilis*, YfkJ and YwlE, which are highly similar to each other in primary structure as well as to LMPTPs from gram-negative bacteria. When purified from overexpressing *Escherichia coli* strains, both enzymes were able to dephosphorylate *p*-nitrophenyl-phosphate and phosphotyrosine-containing substrates in vitro but showed significant differences in kinetic parameters and sensitivity to inhibitors. Transcriptional analyses showed that *yfkJ* was transcribed at a low level throughout the growth cycle and underwent a σ^B-dependent transcriptional upregulation in response to ethanol stress. The transcription of *ywlE* was growth dependent but stress insensitive. Genomic deletion of each phosphatase-encoding gene led to a phenotype of reduced bacterial resistance to ethanol stress, which was more marked in the *ywlE* deletion strain. Our study suggests that YfkJ and YwlE play roles in *B. subtilis* stress resistance.

In higher eukaryotes, protein phosphorylation on tyrosine residues is a key mechanism for cell-cell communication, signal transduction, vesicle traffic, and regulation of cell proliferation and differentiation (21, 36). Tyrosine phosphorylation also plays an important role in many other aspects of cell physiology and embryonic development (14, 21). The human genome contains 90 genes for protein tyrosine kinases (PTKs) and 107 genes for protein tyrosine phosphatases (PTPs) (1).

The study of protein tyrosine phosphorylation in bacteria presents some technical challenges (13). Nevertheless, a number of reports have demonstrated the presence of tyrosine-phosphorylated intracellular proteins in archaea (47), mycobacteria (7), and gram-negative organisms (23, 27, 39, 51). PTKs and PTPs have also been isolated from bacteria (9, 41), suggesting that this posttranslational modification may play an important role in bacterial physiology.

Genome sequencing projects have shown that enzymes similar to eukaryotic PTPs are encoded by many bacteria and archaea (24, 25). Most of the chromosome-encoded PTPs are class I or class II enzymes (1), also known as dual (serine/threonine and tyrosine)-specificity PTPs and low-M_r PTPs (LMPTPs), respectively. Classical class I PTPs, like the plasmid-encoded YopH, which is a virulence factor of *Yersinia pestis* and *Yersinia pseudotuberculosis*, have also been identified

(1, 10). LMPTPs are among the most ancient and highly conserved subfamilies of PTPs. The first bacterial LMPTPs were isolated from *Erwinia amylovora* (5), *Acinetobacter johnsonii* (15), and *Escherichia coli* (54). These enzymes show a remarkably high degree of identity (~30%) with their human homologs.

The physiological functions of bacterial LMPTPs remain largely unknown, although some hints are given by the organization of genes surrounding the PTPs on the chromosome. For example, the gene encoding the AmsI LMPTP of *E. amylovora* is located within the *ams* operon, which controls capsular exopolysaccharide synthesis (5). Similarly, the Ptp LMPTP of *A. johnsonii* can dephosphorylate the transmembrane autokinase Ptk, which regulates the synthesis of colanic acid, a fundamental component of the *Acinetobacter* capsule (15). In fact, control of polysaccharide capsule composition by an autokinase-LMPTP pair encoded in the *cps* or *cps*-like operon has been found to be a conserved feature among gram-negative organisms (55). For example, Wzb, one of the pair of LMPTPs (Wzb and Etp) in *E. coli* (54), as well as one LMPTP from *Klebsiella pneumoniae* (42), dephosphorylate a tyrosine autokinase that regulates capsule composition. However, LMPTP functions in gram-negatives are apparently not limited to the regulation of polysaccharide capsule composition: a recent report by Klein et al. (27) showed that the Etp LMPTP of *E. coli* regulates heat shock resistance by dephosphorylating the sigma factor RpoH and the anti-sigma factor RseA. Interestingly, this function was not shared by the second LMPTP in *E. coli*, Wzb, providing a first example of nonoverlapping functions of LMPTP pairs in bacteria.

TABLE 1. Bacterial strains and plasmids

Strain or plasmid	Description	Source or reference
Strains		
E. coli		
XL10-Gold		Stratagene
BL21(DE3) codonPlus-RIL		Stratagene
B. subtilis		
JH642	*trpC2 pheA1*	Lab stock
JH19000	JH642[a] *sigB::cat*	11
LM58 (Δ*yfkJ*)	JH642::pLM58 *yfkJ*::[*erm* P$_{spac}$*lacZ*]	This study
LM24 (Δ*ywlE*)	JH642::pLM24[a] *ywlE::spc*	This study
LM02	JH642::pLM02[a] *yfkJ::cat*	This study
LM50	LM02::pLM24[a] *yfkJ::cat ywlE::spc*	This study
LM08	JH642::pLM06B *amyE::[yfkJp-lacZ::aph]*	This study
LM14	JH19000::pLM06B *sigB amyE::[yfkJp-lacZ::aph]*	This study
LM35	JH642::pLM35 *amyE::[ywlEp-lacZ::aph]*	This study
LM60	JH19000::pLM35 *sigB amyE::[ywlEp-lacZ::aph]*	This study
Plasmids		
pEGST	GST gene in pET23b (Novagen)	26
pET15b	Cleavable N terminus His$_6$ tag	Novagen
pJM134A	Spectinomycin cassette in pBluescriptIIKS (+)	Unpublished
pMUTIN2	P$_{spac}$*lacZ* + erythromycin cassette	32
pJM115	*lacZ* transcriptional fusion that integrates in *amyE*	40
pLM58	Construct for nonpolar deletion of *yfkJ* in pMUTIN2	This study
pLM24	Left and right arms of *ywlE* in pJM134	This study
pLM02	Left and right arms of *yfkJ* in pJM105A	This study
pLM06B	*yfkJ* promoter in pJM115	This study
pLM35	*ywlE* promoter in pJM115	This study

[a] This strain was transformed with linearized plasmids.

LMPTPs have recently also been found in gram-positive organisms (48), but it is not yet known if these enzymes have functions similar to those of their homologs in gram-negative bacteria. Although the regulation of capsular composition by an autokinase/PTP pair seems to occur in *Streptococcus pneumoniae* and *Staphylococcus aureus* (3, 34, 46), it was found that the PTP encoded by the *cps* operon of *S. pneumoniae* belongs to an unrelated family of Mn^{2+}-dependent PTPs (35) rather than being an LMPTP. The first PTP isolated from *B. subtilis*, YwqE, is also a Mn^{2+}-dependent enzyme and is located in a *cps*-like operon. Within this operon, YwqE is able to dephosphorylate the tyrosine autokinase YwqD and the kinase substrate YwqF, which is a UDP-glucose dehydrogenase (30, 32).

In the present study we report the genetic and biochemical characterizations of two *B. subtilis* LMPTPs, YfkJ and YwlE. The two enzymes are active as PTPs in vitro but show significant differences in their biochemical properties. Deletion of the corresponding coding genes affected *B. subtilis* resistance to ethanol stress.

MATERIALS AND METHODS

Bioinformatic and statistical analyses. BLAST searches and amino acid sequence comparisons were performed using the NCBI site (http://www.ncbi.nlm.nih.gov/BLAST/). Genomic context analysis was performed using SEED (http://theseed.uchicago.edu/FIG/index.cgi), a genomic database and annotation platform provided by the Fellowship for Interpretation of Genomes. This software supports a comparative genome context analysis across a collection of ~300 complete (or almost complete) genomes (38). Experimental errors were evaluated according to the method of J. R. Taylor (50) using the Excel X for Mac software (Microsoft Corporation).

Reagents. *Pfu* Turbo was from Stratagene (La Jolla, CA). BIOMOL GREEN reagent was purchased from Biomol Research Labs (Plymouth Meeting, PA).

Tyrosine phosphopeptides were provided by E. Ruoslahti (The Burnham Institute), and the serine and threonine phosphopeptides were purchased from Upstate (Charlottesville, VA). All other reagents were from ICN Biomedicals (Irvine, CA) or Sigma (St. Louis, MO) unless otherwise stated.

B. subtilis culture and physiological assays. Transformation of *B. subtilis* was performed as described by Anagnostopoulos and Spizizen (2). Liquid cultures of *B. subtilis* were performed in Luria-Bertani (LB) medium or in Schaeffer's sporulation medium (SM) (17). Induction of transcription by ethanol (EtOH) stress was analyzed by following the procedure described by Price et al., using 5% EtOH (43). EtOH survival assays were carried out as described by Völker et al. (56) with slight modifications. Cells were grown overnight at 37°C in LB agar and then inoculated in LB medium and grown at 37°C to an optical density at 540 nm of 0.3 to 0.4, at which time EtOH was added to a final concentration of 9% (vol/vol). The specific growth rate of the culture was monitored before and after the stress. Aliquots of the culture were sampled at 30, 60, 90, 180, and 260 min, and appropriate dilutions were plated in duplicate on LB agar to determine cell viability. Survival was calculated as a ratio between the average number of colonies at the indicated times and the number of colonies at time zero (11, 56). For analysis of motility, *B. subtilis* strains were spotted onto a semisolid plates of tryptone (1.0 g tryptone, 0.5 g NaCl, 0.27 g agar in 100 ml water; after sterilization, 1 ml of 10× Spizizen salts, 5 μg/ml tryptophan, and 5 μg/ml phenylalanine were added to the media) and CK's proline (0.25 g agar was solubilized in 100 ml water and sterilized before the addition of 1 ml of 10× Spizizen salts, 5 μg/ml tryptophan, 5 μg/ml phenylalanine, 0.7 mM sorbitol, and 0.2 mM proline) (28, 59). As the bacteria metabolize nutrients, a chemical gradient is established, resulting in the formation of a ring as the bacteria tax outwards. Differences in the swarm diameters show diversity in strain motility. *B. subtilis* strains were tested for α-amylase and protease activity by growing them on TBAB (tryptose blood agar base; Difco) starch and TBAB milk plates, respectively, prepared as described previously (17). Antibiotic selection in *B. subtilis* strains was carried out at the following concentrations: for chloramphenicol, 5 μg/ml; for kanamycin, 2 μg/ml; for spectinomycin, 50 μg/ml; and for erythromycin, 1 μg/ml plus lyncomycin at 25 μg/ml.

Construction of B. subtilis strains and isolation of recombinant proteins. *B. subtilis* strains and plasmids used are listed in Table 1. Primers used in the study are listed in Table 2. Site-directed mutagenesis was performed using the Quick-Change site-directed mutagenesis kit (Stratagene, La Jolla, CA) according to the

manufacturer's recommendations. All mutations were verified by nucleotide sequencing. Genomic DNA from *B. subtilis* strain JH642 was used as the template for PCR amplifications. The *yfkJ* coding sequence was cloned between the BamHI and HindIII sites of the pEGST vector (primers FKJBAM-F and FKJHIN-R), which allows the expression of proteins with an N-terminal glutathione *S*-transferase (GST) tag (26). The same *yfkJ* fragment and the *ywlE* coding sequence were also cloned between the NdeI and XhoI sites of the pET15b vector (Novagen, Madison, WI) (primers KJNDE-F and KJXHO-R for *yfkJ* and WLENDE-F and WLEXHO-R for *ywlE*) in order to express the proteins with an N-terminal His$_6$ tag.

A nonpolar deletion of *yfkJ* (strain LM58 [$\Delta yfkJ$]) was achieved by single-crossover integration of a plasmid constructed using the vector pMUTIN2, carrying a 330-bp *yfkJ* internal fragment cloned between HindIII and BamHI (primers MUTKJHIND-FW and MUTKJBAM-RV) and an erythromycin resistance cassette (32). Integration of the plasmid caused disruption of *yfkJ* expression, while expression of the genes 3′ to *yfkJ* in the same operon (*yfkI* and *yfkH*) was placed under the control of the IPTG (isopropyl-β-D-thiogalactopyranoside)-inducible P$_{spac}$ promoter. A polar deletion of *yfkJ* (strain LM02) was achieved by double-crossover integration of a plasmid constructed using the vector pJM105A (40), which replaced 446 bp within the *yfkJ* gene with a chloramphenicol cassette. The right arm was cloned between the HindIII and KpnI sites (primers JRIGHT-HIND-F and JRIGHTKPN-R), while the left arm was cloned between the SacI and PstI sites (primers JLEFTSAC-F and JLEFTPST-R). The genomic deletion of *ywlE* (strain LM24 [$\Delta ywlE$]) was achieved by double-crossover integration of a plasmid constructed using the vector pJM134A (M. Perego, unpublished data), which replaced 426 bp within the *ywlE* gene with a spectinomycin cassette carrying a terminator. The right arm was cloned between the HindIII and KpnI sites (primers WLEHIND5′ and WLEKPN3′), while the left arm was cloned between the PstI and EcoRI sites (primers WLEBAM5′ and WLEECO3′). A *B. subtilis* strain carrying a double deletion of *yfkJ* and *ywlE* was also generated by transformation of the LM02 strain with the DNA construct used for generating the $\Delta ywlE$ deletion strain. Diagnostic PCRs were carried out to ensure plasmid integration within the *yfkJ* operon or deletion of *yfkJ* or *ywlE*.

The promoter regions of *yfkJ* (from nucleotide [nt] −255 to nt +12 from the ATG codon) and *ywlE* (from nt −387 to nt +33 from the ATG codon) were cloned, respectively, in the SmaI site and between the EcoRI and BamHI sites of the vector pJM115 (40) (primers YFKJ5′SAC2 and JLEFTPST-R for *yfkJp* and primers WLEPROMECO-FW and WLEPROMBAM-RV for *ywlEp*), which allows the expression of a transcriptional fusion with *E. coli* β-galactosidase upon integration via double crossover at the *amyE* gene of the *B. subtilis* chromosome.

Isolation of GST- or His$_6$-tagged recombinant proteins was performed by single-step affinity chromatography using glutathione Sepharose 4B (Amersham Biosciences, Piscataway, NJ) or Ni-nitrilotriacetic acid (NTA) agarose (QIAGEN Inc., Valencia, CA), respectively. The purity of recombinant proteins was consistently over 95%, as determined by Coomassie blue staining of gels.

Phosphopeptides and phosphosubstrate dephosphorylation assays. Dephosphorylation of phosphopeptides and other phosphorylated compounds was carried out at 37°C in a 50- or 100-μl total volume. For YfkJ, the reaction buffer was 50 mM sodium citrate, pH 6.0, or 50 mM Bis-Tris, pH 6.0. The substrate hydrolysis rate was measured either by reading the *p*-nitrophenol absorbance at 405 nm after the addition of 200 μl of 1 M NaOH to the reaction mixture and using the extinction coefficient of 18.000 M^{-1} cm^{-1} for *p*-nitrophenol or by reading the absorbance at 620 nm after the addition of 100 to 200 μl of BIOMOL GREEN reagent to the reaction mixture and calculating the release of inorganic phosphate by comparison with a standard curve of inorganic phosphate. The nonenzymatic hydrolysis of the substrate was corrected by measuring the control without addition of enzyme. For YwlE, the reaction buffer was 50 mM MES (pH 5.5), 1 mM dithiothreitol (DTT) and the hydrolysis rate was always measured by the addition of BIOMOL GREEN reagent. Absorbance readings were carried out on a PowerWaveX340 microplate spectrophotometer (Bio-Tek Instruments, Inc., Winooski, VT). The time of the reaction, amount of enzyme, and concentration of the substrate were optimized to have a linear kinetics. The initial hydrolysis rate (v^0) was measured in triplicate for *p*-nitrophenyl-phosphate (*p*NPP) and in duplicate for phosphopeptides.

Kinetic parameters were determined by fitting the data to the Michaelis-Menten equation or to the Michaelis-Menten with substrate (*S*) inhibition equation: $v^0 = V_{max}[S]/\{K_m + [S](1 + [S]/K_i)\}$ (see http://www.lsbu.ac.uk/biology/enztech/inhibition.html), using nonlinear regression and the Prism software (GraphPad Prism version 4.00 for Mac OS X; GraphPad Software, San Diego, CA). The K_i for vanadate was evaluated by fitting the data to the Michaelis-Menten equation for competitive inhibition: $v^0 = V_{max}[S]/(K_{Mapp} + [S])$, where K_{Mapp} is $K_m(1 + [I]/K_i)$ (where [*I*] is the concentration of the inhibitor, in molar units) using the same software.

Purification and dephosphorylation of Spo0F~P and Spo0B~P. His$_6$-Spo0F (50 μM) was phosphorylated with KinA (0.5 μM) and [γ-^{32}P]ATP (0.3 μM at a specific activity of 6,000 Ci/mmol) in the phosphorelay buffer (50 mM EPPS [4-(2-hydroxyethyl)piperazine-1-propanesulfonic acid], pH 8.5, 20 mM MgCl$_2$, 0.1 mM EDTA, 5% glycerol) for 1 h at room temperature. ATP was added to a final concentration of 1 mM, and the phosphotransfer was continued for another hour (52). Spo0F~P was purified by using Ni-NTA agarose equilibrated with binding buffer (50 mM Tris-HCl, pH 8, 300 mM NaCl, 10 mM imidazole, 5 mM β-mercaptoethanol). The column was washed with 10 ml of binding buffer, and protein elution was obtained with binding buffer containing 150 mM EDTA. Fractions containing radioactivity were dialyzed in 20 mM HEPES-NaOH, pH 7.0, 0.1 mM EDTA, 10% glycerol. Aliquots were stored at −80°C. The ratio of Spo0F to Spo0F~P in the purified sample was determined by analysis on a 10% Tris-glycine native polyacrylamide gel electrophoresis gel stained with Coomassie blue. The concentration of Spo0F/Spo0F~P used throughout this study refers to the fraction of Spo0F~P only.

His$_6$-Spo0B (100 μM) was labeled in a 250-μl reaction mixture containing KinA (10 μM), Spo0F (100 μM), and [γ-^{32}P]ATP (0.3 μM at a specific activity of 6,000 Ci/mmol) in the phosphorelay buffer (50 mM EPPS, pH 8.5, 20 mM MgCl$_2$, 0.1 mM EDTA, 5% glycerol) for 1 h at room temperature. ATP was added to a final concentration of 1 mM, and the phosphotransfer was continued for another hour (53). The reaction was mixed with Ni-NTA agarose equilibrated with binding buffer containing 20 mM Tris-HCl, pH 7.4, 50 mM KCl, 5 mM imidazole, and 5 mM β-mercaptoethanol. Two additional washes with binding buffer containing 10 mM imidazole were carried out before the protein was eluted in buffer containing 20 mM Tris-HCl, pH 7.4, 50 mM KCl, 250 mM imidazole, and 5 mM β-mercaptoethanol. Fractions (500 μl) were collected, and 4 μl of each was run on a 15% sodium dodecyl sulfate (SDS)-acrylamide gel. The gel was directly exposed to a PhosphorImager screen (Molecular Dynamics/Amersham Biosciences, Piscataway, NJ) and analyzed after 1 h of exposure. Fractions containing radioactivity were dialyzed in 20 mM Tris-HCl, pH 7.4, 0.1 mM EDTA, 1 mM DTT and concentrated using a Centricon-10 concentrator (Amicon/Millipore, Bedford, MA). Protein concentration was determined with a Bradford-based Bio-Rad protein assay (Bio-Rad Laboratories, Hercules, CA).

The dephosphorylation assay used to test YwlE and YfkJ activity on Spo0F~P and Spo0B~P was carried out at 37°C in a reaction buffer containing 50 mM HEPES-NaOH, pH 7.0, 2 mM EDTA, 1 mM DTT. A time course assay was done in which His-YwlE (1.5 μM) or GST-YfkJ (1.5 μM) was incubated with 1.5 μM Spo0F~P or Spo0B~P. Control reactions were performed using Spo0F~P or Spo0B~P in the reaction buffer in the absence of the phosphatase. At the time points indicated in the figure, 15 μl of samples was withdrawn and the reactions were stopped by the addition of 3 μl 5× SDS loading buffer (25 mM Tris-HCl, pH 6.8, 1.5% SDS, 5% β-mercaptoethanol, 10% glycerol, 0.02% bromophenol blue). Samples were loaded onto 15% SDS–PAGE. Electrophoresis was carried out at constant voltage (100 V) for 2 h. The gels were dried and exposed overnight to a PhosphorImager screen and then analyzed with Image Quant software (Molecular Dynamics/Amersham Biosciences, Piscataway, NJ).

β-Galactosidase assay. β-Galactosidase assays were performed as described previously (12). Cultures were grown in LB medium or SM. Samples were taken at the stated intervals, and the activities are expressed in Miller units (33).

RT-PCR. RNA was extracted from strains JH642, LM58 ($\Delta yfkJ$), and LM24 ($\Delta ywlE$) grown in 3 ml LB medium overnight at 37°C using the RNAqueous kit from Ambion (Austin, TX). Turbo-DNase (Ambion, Austin, TX) was added to each RNA preparation at a final concentration of 0.05 U/μg RNA/μl for 1 h at 37°C and then inactivated by addition of EDTA to a final concentration of 5 mM and heating the mixture at 75°C for 10 min. The amount of extracted RNA was determined by measuring its absorbance at 260 nm. Reverse transcription (RT) was performed on 400 ng RNA, starting from nt +337 from the ATG of *yfkH* or from nt +1060 from the ATG of *ywlE*, using the primer H3′ or LFRV, respectively, and ImPromII reverse transcriptase (Promega, Madison, WI). PCRs on the RT products were performed using primers KJNDE-FW and KJXHO-RV for *yfkJ*, 64F and 63R for *yfkIH*, and YWLF-FW and YWLF-RV for *ywlF*, with AmpliTaq polymerase (Roche, Basel, Switzerland). PCR performed using equal amounts of nonretrotranscribed RNA was used as a control for genomic DNA contamination of the RNA samples.

RESULTS

Bioinformatic analysis of *B. subtilis* LMPTPs. A BLAST analysis of the completed and annotated *B. subtilis* genome (29) was carried out using the human LMPTP-A tyrosine phosphatase as the query sequence. Two genes were identified, *yfkJ*

```
YfkJ     (B.subtilis)  -----MISVLFVCLGNICRSPMAEAIFRDLAAKKGLEGKIKADSAG-IGGWHIGNPPHEG  54
YwlE     (B.subtilis)  ------MDIIFVCTGNTCRSPMAEALFKSIAEREGLNVNVRSAG---VFASPNGK-ATPH  50
PtpA     (S.aureus)    -----MVDVAFVCLGNICRSPMAEAIMRQRLKDRNIH-DIKVHSRG-TGSWNLGEPPHEG  53
Wzb      (E.coli)      ----MFNNILVVCVGNICRSPTAERLLQRYHPELKVESAG--------LGALVGKGADPT  48
Stp1     (S.pombe)     --MTKNIQVLFVCLGNICRSPMAEAVFRNEVEKAGLEARFDTIDSCGTGAWHVGNRPDPR  58
LMPTP-A  (H.sapiens)   MAEQATKSVLFVCLGNICRSPIAEAVFRKLVTDQNISENW-RVDSAATSGYEIGNPPDYR  59
LMPTP-B  (H.sapiens)   MAEQATKSVLFVCLGNICRSPIAEAVFRKLVTDQNISENW-VIDSGAVSDWNVGRSPDPR  58


YfkJ     (B.subtilis)  TQEILRREGISFDGMLARQVSEQDLDDFDYIIAMDAENIGSLR--SMAGFKNTSHIKRLL  112
YwlE     (B.subtilis)  AVEALFEKHIALN-HVSSPLTEELMESADLVLAMTHQHKQIIA---SQFGRYRDKVFTLK  106
PtpA     (S.aureus)    TQKILNKHNIPFDGMISELFEAT--DDFDYIVAMDQSNVDNIK--SIN-PNLKGQLFKLL  108
Wzb      (E.coli)      AISVAAEHQLSLEGHCARQISRRLCRNYDLILTMEKRHIERLC---EMAPEMRGKVMLFG  105
Stp1     (S.pombe)     TLEVLKKNGIHTK-HLARKLSTSDFKNFDYIFAMDSSNLRNINRVKPQGS--RAKVMLFG  115
LMPTP-A  (H.sapiens)   GQSCMKRHGIPMS-HVARQITKEDFATFDYILCMDESNLRDLNRKSNQVKTCKAKIELLG  118
LMPTP-B  (H.sapiens)   AVSCLRNHGIHTA-HKARQITKEDFATFDYILCMDESNLRDLNRKSNQVKTCKAKIELLG  117


YfkJ     (B.subtilis)  DYVEDSDLADVEDPYYTGN--FEEVCQLIKTGCEQLLASIQKEKQL---  156
YwlE     (B.subtilis)  EYV-TGSHGDVLDPFGGSIDIYKQTRDELEELLRQLAKQLKKDRR----  150
PtpA     (S.aureus)    EFS-NMEESDVEDPYYTNN--FEGVYDMVLSSCDNLIDYIVKDANLKEG  154
Wzb      (E.coli)      HWD---NECEIEDPYRKSRETFAAVYTLLERSARQWAQALNAEQV----  147
Stp1     (S.pombe)     EYASPGVSKIVDDPYYGGSDGFGDCYIQLVDFSQNFLKSIA-------  156
LMPTP-A  (H.sapiens)   SYD-PQKQLIIEDPYYGNDSDFETVYQQCVRCCRAFLEKAH-------  158
LMPTP-B  (H.sapiens)   SYD-PQKQLIIEDPYYGNDSDFETVYQQCVRCCRAFLEKAH-------  157
```

FIG. 1. Amino acid sequence alignment of *B. subtilis* YfkJ and YwlE with LMPTPs from prokaryotic and eukaryotic organisms. Amino acid residues that are conserved in all the considered species are in bold. The boxes indicate the catalytic motifs referred to in the text.

and *ywlE*, predicted to encode proteins with high degrees of amino acid identity to LMPTP-A (39% [E = 10^{-20}] and 26% [E = 2×10^{-6}], respectively). Additionally, YfkJ and YwlE showed a 29% amino acid identity and 53% similarity (E = 9 $\times 10^{-8}$) to each other (the matrix used was BLOSUM62). An amino acid sequence alignment of YfkJ and YwlE with other prokaryotic and eukaryotic LMPTPs is shown in Fig. 1. Two amino acid sequence motifs are conserved in all LMPTPs: the CXGNXCR stretch at the N terminus defines the P-loop of LMPTPs and corresponds to the CX_5R motif in all PTPs (44), while the DP motif is part of the phosphatase D-loop and is followed by two tyrosines in nearly all LMPTPs (44, 58).

Our BLAST search revealed the presence of an additional gene with a lower degree of similarity to the human LMPTPs. This protein is a low-molecular-weight arsenate reductase (*arsC*/*yqcM*) and is known to have a similar fold but a quite different catalytic mechanism and extremely weak phosphatase activity in vitro (4). We also found that YfkJ and YwlE are included in a single cluster of orthologs (COG) (49) available at the website http://www.ncbi.nlm.nih.gov/cgi-bin/COG/palox?COG0394. On a similarity tree (also available at the same website), based on multiple sequence alignments of all proteins belonging to the COG, YwlE appears to be distant from YfkJ, and both *B. subtilis* enzymes are distant from the *E. coli* LMPTPs.

On the *B. subtilis* annotated chromosome, *yfkJ* seems to be the first of a putative three-gene operon (*yfkJ*, *yfkI*, and *yfkH*), while *ywlE* seems to form an operon with the genes *ywlC*, *ywlD*, *ywlF*, and *ywlG* (29). We performed for the two genes a genome context analysis, including clustering of genes on the chromosome, domain fusions, and cooccurrence profiles. Such analyses often provide important clues to cellular functions of genes (38). A genome context analysis of *yfkJ* (illustrated in Fig. S1 of the supplemental material) revealed that homologs of genes encoding the inducible RNase BN (*yfkH*), described for *E. coli* (6), and a small conserved protein of unknown function (*yfkK*) have a strong tendency to cooccur in the genomic neighborhood of *yfkJ*. This tendency is observed over a broad range of gram-positive bacteria, including most of the sequenced species of *Bacillus* and *Staphylococcus aureus*. *yfkH* and *yfkK* genes are clustered on the chromosome in all sequenced strains of *Listeria* spp., where *yfkJ* orthologs are present in a remote locus. All three genes, *yfkJ*, *yfkH*, and *yfkK*, are conserved but dispersed over the chromosome of *Bacillus halodurans*. On the other hand, homologs of *yfkI* (for which there is no known function) are present (and coclustered) only in a compact group, including in *Bacillus anthracis*, *Bacillus cereus*, and *Bacillus thuringiensis*.

A genome context analysis performed for *ywlE* revealed an extensive pattern of conservation and possible functional coupling (illustrated in Fig. S2 of the supplemental material). A conserved chromosomal cluster containing *ywlE* extends well beyond the boundaries of a possible *ywl* operon. Distal genes *prfA* and *hemK*, as well as *ywlC*, are the most conserved components of this cluster, as detected in a total of 28 sequenced genomes of rather divergent gram-positive bacteria, including all sequenced species of *Bacillus*, *Staphylococcus*, *Listeria*, and *Clostridium* and of *Moorella thermoacetica*, *Exiguobacterium* sp., and *Thermoanaerobacter tengcongensis*. Interestingly, all three genes are united by a common "theme"—ribosome and translation. The gene *hemK* encodes an essential and widely conserved N^5-glutamine methyltransferase, which modifies peptide release factors, including the one encoded by its conserved chromosomal neighbor, the essential gene *prfA* (18). Although a precise function of *ywlC* (widely conserved in many bacteria) is not known, its homolog SUA5 is an essential gene
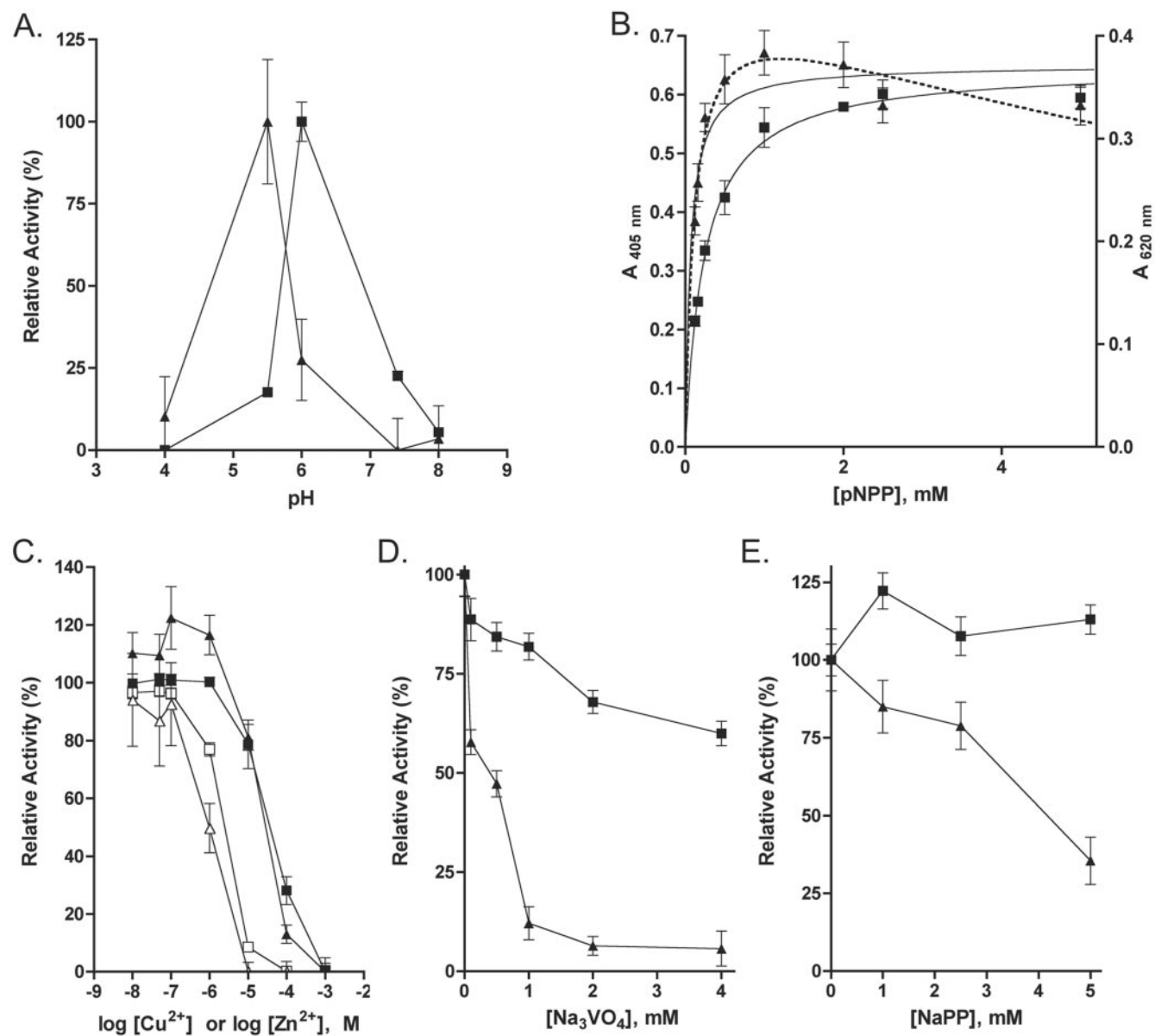
FIG. 2. Biochemical characterization of *B. subtilis* YfkJ and YwlE enzymatic activity using *p*NPP as the substrate. (A) Effect of pH on YfkJ (squares) and YwlE (triangles) enzymatic activities. The assays contained 3 mM *p*NPP as the substrate. Buffers used were sodium citrate (pHs 4.0 and 6.0), MES-NaOH (pH 5.5), and Tris-HCl (pHs 7.4 and 8.0). Data represent relative activities. (B) Analysis of YfkJ (squares) and YwlE (triangles) enzymatic activities using *p*NPP as the substrate. The graphs represent mean activities and nonlinear fits of the experimental data to the Michaelis-Menten equation (continuous lines). The dotted line is a nonlinear fit of YwlE data to the Michaelis-Menten equation for substrate inhibition (see http://www.lsbu.ac.uk/biology/enztech/inhibition.html). (C, D, E) Effect of $CuCl_2$ (C, open symbols), $ZnCl_2$ (C, filled symbols), Na_3VO_4 (D), and sodium pyrophosphate (E) on YfkJ (squares) and YwlE (triangles) enzymatic activities. The buffer used for YfkJ was 50 mM sodium citrate or 50 mM Bis-Tris (pH 6.0), and the buffer used for YwlE was 50 mM MES (pH 5.5), 1 mM DTT. The assays contained 3 mM *p*NPP as the substrate, and data represent relative activities. Error bars in all graphs represent standard errors; if not visible, they are within the resolution of the point.

in *Saccharomyces cerevisiae* implicated in the regulation of translation (37). Among other less conserved components of the cluster are three metabolic enzymes (YwlF [ribose 5-phosphate isomerase], GlyA [serine hydroxymethyltransferase], and Upp [uracil phosphoribosyltransferase]) and two proteins of unknown function (encoded by *ywlD* and *ywlG*). Notably, *upp*, often located immediately downstream of *ywlE*, forms a bifunctional fusion, YwlE-Upp, in *T. tengcongensis*. Finally, the

spoIIR gene, involved in the regulation of stage II sporulation, is coclustered with *ywlE* only in a subset of *Bacillus* subspp.

Biochemical characterization of recombinant *B. subtilis* LMPTPs. To first characterize the two *B. subtilis* LMPTPs in vitro, we cloned their genes into *E. coli* expression vectors. YwlE was purified as a His_6-tagged protein, while YfkJ was purified both as a His_6 and as an N-terminal GST fusion protein from *E. coli* lysates. The phosphatase activity of *B.*

TABLE 2. Primers used in this study

Primer	Sequence[a]
FKJBAM-F	CG**GGATCC**ATGATAAGCGTGTTATTTGTTTG
FKJHIN-R	CCC**AAGCTT**CACAATTGTTTTTCTTTTTG
KJNDE-F	GGAATTC**CATATG**ATAAGCGTGTTATTTGTTTG
KJXHO-R	CCGC**TCGAG**TCACAATTGTTTTTCTTTTTGAATG
WLENDE-F	GGAATTC**CATATG**GATATTATTTTTGTCTGTACTG
WLEXHO-R	CCG**CTCGAG**TTATCTACGGTCTTTTTTCAGC
MUTKJHIND-FW	CCC**AAGCTT**TCTCCGATGGCGGAAGC
MUTKJBAM-RV	CG**GGATCC**CGGGTACGTCAGCCAG
JRIGHTHIND-F	CCC**AAGCTT**GTGAAAGGAGAATTTGCATG
JRIGHTKPN-R	CGG**GGTACC**CCTTCATGAAGGGTGTATC
JLEFTSAC-F	GCAT**GAGCTC**GGGAAATGATAAAAAAGACTCG
JLEFTPST-R	GCAT**CTGCAG**GATGTGCAACCTCCCTATTC
WLEHIND-5'	CCC**AAGCTT**GACCGTAGATAAGTTGTCAG
WLEKPN-3'	A**CCCGGG**TACCCATCGCAAGG
WLEBAM-5'	GGATG**GGATCC**GGTAACATGCTGTC
WLEECO-3'	AAAAA**GAATT**CCCATGTCAGTCAC
YFKJ5'SAC2	TGGG**AGAGCTC**TTCAATCATTTGAGTTAATG
JLEFTPST-R	GCAT**CTGCAG**GATGTGCAACCTCCCTATTC
WLEPROMECO-FW	CG**GAATTC**GTTCTTGGGGGTTCAAATG
WLEPROMBAM-RV	CG**GGATCC**CGTATTTCCAGTACAGAC
H3	CCGGACGATCGCATTC
LFRV	CTACAGGTTTTTCTCTTCAT
64F	AAACAACGCCGCAAGTGATG
63R	GGCGATAATCCCGAATGACA
YWLF-FW	GTAGCCATTGCATCGGATC
YWLF-RV	CGCGTTTGGTGTCTTCCC
KJC8SAVR-F	GATAAGCGTGTTATTTGTTTCCCTAGGTAACATTTGCCG
KJC8SAVR-R	CGGCAAATGTTACCTAGGGAAACAAATAACACGCTTATC
KJD125ABSP-F	GATCTGGCTGACGTACCTGCTCCTTACTACACAGGGAAC
KJD125ABSP-R	GTTCCCTGTGTAGTAAGGAGCAGGTACGTCAGCCAGATC
YFKJR14KNDE-F	GTTTGTTTAGGTAACATATGCCAAGTCTCCGATGGCG
YFKJR14KNDE-R	CGCCATCGGAGACTTGCATATGTTACCTAAACAAAC
WLEC8SAGEI-F	ATGGATATTATTTTTGTCTCTACCGGTAATACGTGCCGC
WLEC8SAGEI-R	GCGGCACGTATTACCGGTAGAGACAAAAATAATATCCAT
WLED118ANHEI-F	CATGGTGATGTGCTAGCTCCGTTCGGCGGCTCAATTGAC
WLED118ANHEI-R	GTCAATTGAGCCGCCGAACGGAGCTAGCACATCACCATG
WLER13KBSPMI-F	ACTGGAAATACCTGCAAGAGCCCAATGGCTGAGGCGC
WLER13KBSPMI-R	GCGCCTCAGCCATTGGGCTCTTGCAGGTATTTCCAGT

[a] Restriction sites used for cloning purposes are in bold.

subtilis LMPTPs was then measured using *p*NPP as the substrate. The pH optima for His-YfkJ and His-YwlE were 6.0 and 5.5, respectively (Fig. 2A). Inclusion of 1 mM DTT significantly improved the activity of YwlE (data not shown). Both YfkJ and YwlE dephosphorylated *p*NPP according to Michaelis-Menten kinetics (Fig. 2B), but YwlE was inhibited by a high concentration of the substrate. The K_m values were found to be 0.244 ± 0.009 mM for His-YfkJ and 0.157 ± 0.024 mM for His-YwlE, respectively. These values are comparable to those reported for *S. aureus* PtpA and PtpB (48) and consistent with those reported for several eukaryotic and prokaryotic Cys-based PTPs and for eukaryotic class IV PTPs (a newly isolated class of metal-dependent and non-Cys-based eukaryotic PTPs) (8, 15, 20, 45). The rate constants (k_{cat}) were calculated to be 0.640 ± 0.006 s^{-1} for His-YfkJ and 0.010 ± 0.001 s^{-1} for His-YwlE, which are similar, respectively, to the reported k_{cat} of *S. aureus* PtpA and PtpB for *p*NPP (48). We noticed that the activities of *S. aureus* and *B. subtilis* LMPTPs on *p*NPP appear to be several orders of magnitude lower than those of several eukaryotic PTPs or some gram-negative PTPs (8, 15, 20, 45).

Both Cu^{2+} and Zn^{2+} efficiently inhibited the activity of YfkJ and YwlE (Fig. 2C), while the addition of Mg^{2+}, Ca^{2+}, or Fe^{3+} to the reaction buffer had minimal effects on both phospha-

tases even at 5 mM (data not shown). YfkJ and YwlE were differently sensitive to Na$_3$VO$_4$, a classic PTP competitive inhibitor: while it inhibited YwlE in a competitive manner, with a K_i of 224 nM, YfkJ was insensitive to this inhibitor (Fig. 2D and data not shown). The serine phosphatase inhibitors NaF and NaPP did not inhibit YfkJ, while YwlE was insensitive to NaF but was significantly inhibited by 5 mM NaPP (data not shown and Fig. 2E). In contrast, 5 mM NEM completely inhibited both enzymes, while 5 mM iodoacetamide reduced the activity of YfkJ by 65% and of YwlE by 79% (data not shown).

The enzymes were then assayed using phosphoamino acids, phosphopeptides, and other phosphorylated compounds as substrates. For comparison, we included the human LMPTP-A and -B enzymes, which are considered to be tyrosine-specific enzymes in vitro and in vivo (44). YfkJ showed modest activity on phosphotyrosine but was unable to dephosphorylate a phosphotyrosine-containing peptide modeled after the C terminus of the mammalian tyrosine kinase Lck (Table 2). YwlE, on the other hand, was as active against phosphotyrosine as human LMPTP-B and was even more active against several tyrosine phosphopeptides (Table 2). Neither of the two enzymes were active on phosphoserine- or phosphothreonine-containing substrates. The two bacterial LMPTPs and the two human en-

TABLE 3. Substrate analysis of YfkJ and YwlE

Substrate[b]	Activity of enzyme (Miller units)[a]			
	YfkJ	YwlE	LMPTP-A	LMPTP-B
*p*NPP	100	100	100	100
FTATEGQpYQPQP	0	18.1	61.7	17.1
FTATEGQpYQPIP	0	7.6	41.3	12.6
FTATEGQpYQEIP	0.4	31.8	65.3	18.8
FTATEGQpYEEIP	0.1	36.9	43.2	12.1
RRApSVA	0	0	2.9	4.0
KRpTIRR	0	0	3.8	1.6
p-Tyr	2.3	13.2	82.7	26.6
p-Ser	0	3.6	6.2	3.8
p-Thr	0	0	0	0
α-Naphthyl phosphate	0.6	3.5	4.5	1.2
β-Naphthyl phosphate	21.7	69.9	102.4	98.1
Glucose-1-phosphate	0	20.8	7.3	5.4
Glucose-6-phosphate	0	0	1.4	0
Ribose-5-phosphate	0	0	8.8	0
β-Glycerol phosphate	0	0	0.4	0
Pyridoxal 5′ Phosphate	0	0	0	0
IMP	0.9	4.7	2.1	1.2
ATP	0	0	0.5	0
ADP	0	0	0	0
AMP	0.7	2.1	2.2	0.1
GMP	0.6	2.5	4.2	0
CMP	0.7	2.3	2.8	0.5
UMP	0	0	1.5	1.7

[a] Values are relative activities of *B. subtilis* His-YfkJ and His-YwlE and of human GST–LMPTP-A and GST–LMPTP-B.
[b] The reaction buffer was 50 mM MES (pH 5.5) with 1 mM DTT for His-YwlE or 50 mM Na citrate (pH. 6.0) for the other enzymes. Substrates were present at a 1 mM concentration. pY, phosphotyrosine; pS, phosphoserine; pT, phosphothreonine.

zymes dephosphorylated other phospho-compounds very similarly (Table 2), with the exception of a moderate activity of YwlE against glucose-1-phosphate. Both enzymes were able to dephosphorylate β-naphthyl phosphate but were inactive against α-naphthyl phosphate, which is consistent with our and other reported data on human LMPTPs (57). Neither YfkJ nor YwlE were able to dephosphorylate phospho-Spo0F (previously phosphorylated on Asp-54 by KinA) or phospho-Spo0B (previously phosphorylated on His-30 by phosphate transfer from Spo0F) over a prolonged period of time, suggesting that N-phosphoamino acids are not substrates for the two enzymes (data not shown). Overall, our data are compatible with YwlE and YfkJ being tyrosine-specific phosphatases. The low activity of YfkJ against the phosphotyrosine-containing peptide included in the screen is likely due to a stricter requirement for certain amino acid residues and/or structural determinants surrounding the phosphorylated tyrosine. Alternatively, YfkJ might be specific for a different phosphosubstrate(s) not included in our screen.

Next, we evaluated the role of amino acid residues predicted to be critical for catalysis. Since the GST-YfkJ protein was kinetically identical to His₆-YfkJ against *p*NPP (data not shown), site-directed mutagenesis was performed on the GST-YfkJ construct. Mutation of Cys-8 to Ser, Arg-14 to Lys, or Asp-125 to Ala completely abolished the enzymatic activity of YfkJ. Corresponding mutations of Cys-7, Arg-13, and Asp-118 in YwlE also completely abolished the enzymatic activity (data not shown). Cys-8/-7 and Arg-14/-13 are critical elements of the P-loop (44) and phosphocysteinyl-substrate intermediate

formation, while Asp-125/-118 in the D-loop functions as general base in the catalytic mechanism of LMPTPs (44).

Transcriptional analysis of *B. subtilis* LMPTPs. The promoter region of *yfkJ* includes recognition sequences for both σ^A- and σ^B-dependent transcription (43). By direct DNA array analysis, Price et al. (43) detected an upregulation of *yfkJ* transcription after 5 min of ethanol stress in *B. subtilis*. By rapid amplification of cDNA ends-PCR they also mapped a σ^B-dependent 5′ end of the *yfkJ* mRNA immediately downstream from the putative *yfkJ* σ^B promoter (43). In order to assess whether the 5′-end-flanking regions of *yfkJ* and *ywlE* contain promoter activity and regulate such activity in various growth phases and conditions, we cloned a 255-bp fragment (from nt −255 from *yfkJ* ATG) containing the whole *yfkK-yfkJ* intergenic region and a 420-bp fragment 5′ to *ywlE* ATG (from nt −387 from *ywlE* ATG to nt +33 from *ywlE* ATG, a fragment long enough to include putative *ywlE* promoter sequences) into the transcriptional fusion vector pJM115 (40), thus creating, respectively, the *yfkJ* promoter-*lacZ* and *ywlE* promoter-*lacZ* transcriptional fusion plasmids. The *B. subtilis* strain carrying the *yfkJ* transcriptional fusion showed an overall low β-galactosidase activity in the absence of stress, and for this reason it was analyzed in comparison to a control *B. subtilis* strain transformed with the empty vector alone. Transcription from the *yfkJ* promoter showed a peak of activity in the late exponential phase of growth when bacteria were grown in liquid LB medium (Fig. 3A). When bacteria were grown in sporulation medium, *yfkJ* activity was almost identical to the control throughout the growth cycle (data not shown). Figure 3B shows that ethanol stress, carried out as described by Price et al. using 5% ethanol (43), caused a rapid induction of *yfkJ* transcription. When the experiments were performed in a *B. subtilis* strain that lacks σ^B, the induction of *yfkJ* transcription by ethanol stress was absent, confirming that *yfkJ* transcription is stress inducible and σ^B regulated. The pattern and rates of induction of β-galactosidase activity from the *yfkJ* transcriptional fusion during ethanol stress were compatible with the ones obtained by Price et al. for the *yfkJ* transcript (43).

The β-galactosidase activity of the *ywlE* transcriptional fusion showed a peak in the exponential phase of growth, followed by a significant and gradual reduction in the stationary/sporulation phase (Fig. 3C and D). This pattern was independent from the growth medium, although the activity was much higher when bacteria were grown in SM (Fig. 3D). We did not observe any increase in β-galactosidase activity during ethanol stress (data not shown), suggesting that *ywlE* and *yfkJ* transcriptional regulation might differ in their stress sensitivities. We concluded from these experiments that the 5′-end-flanking regions of both LMPTPs contain sequences necessary for promoter activity. Regulation of these two promoter regions shows significant differences between the two enzymes.

Role of *B. subtilis* LMPTPs in stress resistance. In order to study the physiological role of the two *B. subtilis* LMPTPs, we generated two *B. subtilis* strains carrying a deletion of *yfkJ* or of *ywlE*. To avoid polar effects on *yfkI* and *yfkH*, *yfkJ* was disrupted by integration of a pMUTIN2-based plasmid, which places the transcription of genes downstream from *yfkJ* under the control of an IPTG-inducible promoter (32). The absence of polar effects in our LMPTP deletion strain was confirmed by
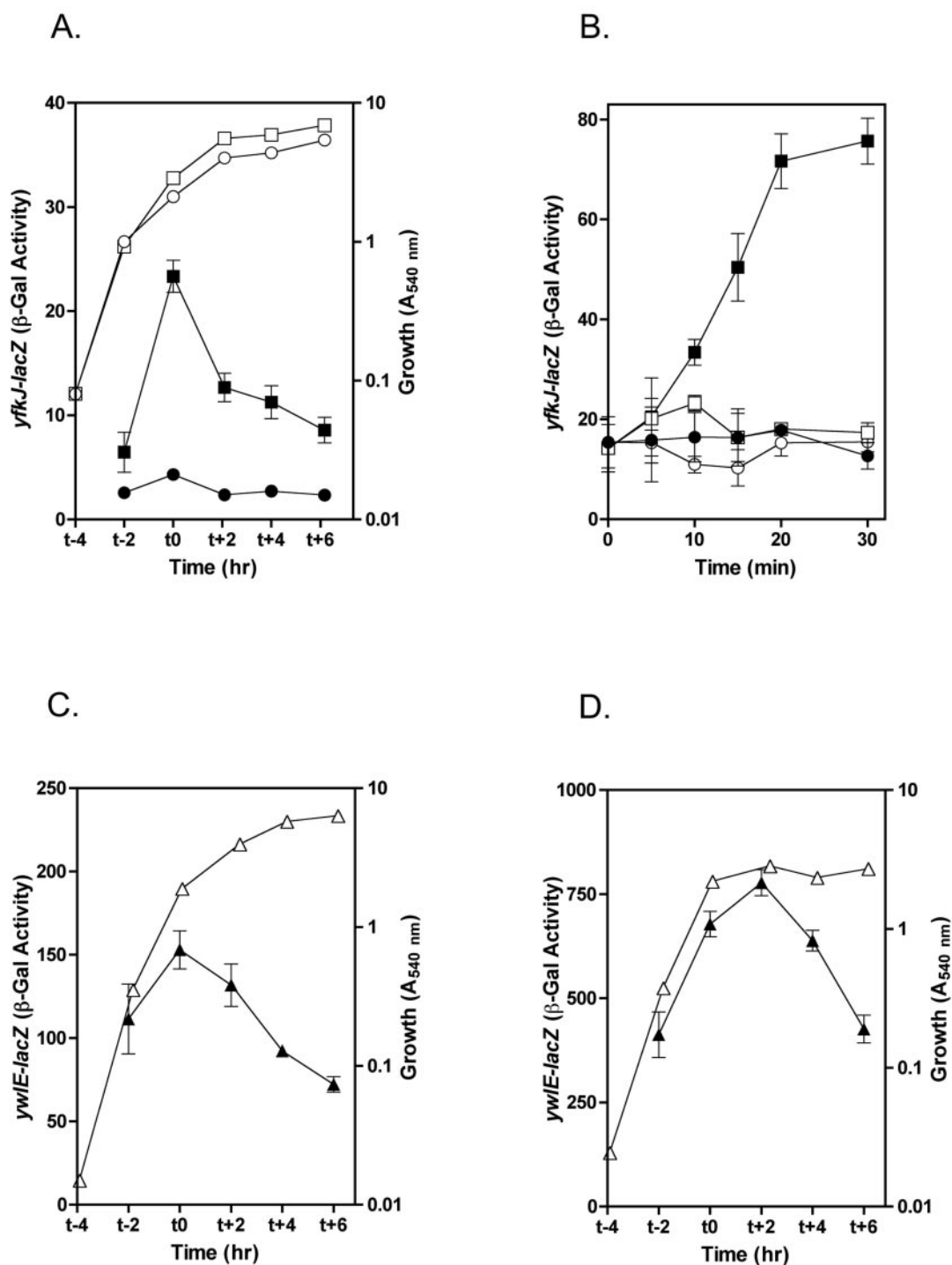
FIG. 3. Transcriptional analysis of *B. subtilis yfkJ* and *ywlE*. (A, C, D) β-Galactosidase activity from *yfkJ* (A) and *ywlE* (C, D) transcriptional fusions during growth in LB medium (A, C) or SM (D). Filled symbols represent β-galactosidase activity expressed in Miller units (33). Open symbols represent average optical densities (540 nm) of bacterial culture at the indicated times. (B) Induction of *yfkJ* transcription by ethanol stress. Ethanol-induced β-galactosidase activity from the *yfkJ* transcriptional fusion in wild-type bacteria (strain LM08 [squares]) or bacteria lacking σ^B (strain LM14 [circles]). Graphs represent β-galactosidase activities expressed in Miller units (33) from bacteria subjected (filled symbols) or not subjected (open symbols) to ethanol treatment. Standard errors have been calculated for all β-galactosidase activity data and reported as error bars. When error bars are not visible, they are within the resolution of the points.
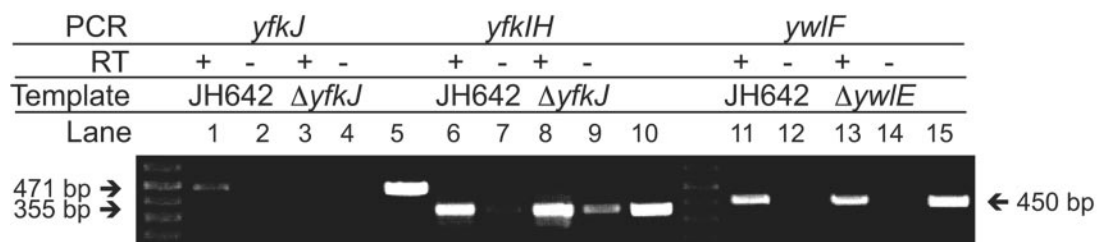
FIG. 4. RT-PCR analysis of JH642, LM58 (Δ*yfkJ*), and LM24 (Δ*ywlE*) *B. subtilis* strains. cDNA was synthesized from total RNA using a reverse primer within *yfkH* (lanes 1 to 9) or within *ywlF* (lanes 11 to 14) and subsequently amplified by PCR using primers within *yfkJ* (lanes 1 to 4), *yfkIH* (lanes 6 to 9), or *ywlF* (lanes 11 to 14). RNA was extracted from lysates of JH642 (lanes 1, 2, 6, 7, 11, and 12) or a Δ*yfkJ* (lanes 3, 4, 8, and 9) or Δ*ywlE* (lanes 13 and 14) strain. Each RT-PCR lane is followed by a control lane for PCR performed using equal amounts of nonretrotranscribed RNA (lanes 2, 4, 7, 9, 12, and 14). Control PCRs are also shown, using genomic DNA of the wild-type JH642 strain as the template and primers within *yfkJ* (lane 5), *yfkIH* (lane 10), or *ywlF* (lane 15). Data shown in lanes 1 to 10 are from bacteria grown in the presence of 1 mM IPTG.

RT-PCR amplification of genes downstream of *yfkJ* and *ywlE*. Figure 4 shows that the transcription of *yfkI* and of *ywlF* was maintained in the Δ*yfkJ* and Δ*ywlE* strains, respectively. Considering the strategies used to generate the deletion strains, these results suggest that the *yfkJ* deletion was nonpolar and that *ywlF* does not form an operon with *ywlE*.

Deletion of one or the other phosphatase did not affect bacterial growth in liquid LB medium or SM at 37°C and in solid SM at 28°C, 37°C, or 50°C (data not shown). The deletion of one or the other phosphatase did not affect protease or amylase production or bacterial motility (data not shown). The σ^B-dependent upregulation of *yfkJ* transcription during ethanol stress prompted us to analyze the role of LMPTPs in the general stress response. Thus, the *B. subtilis* strains carrying deletions of one or the other LMPTPs were analyzed for their ability to respond to ethanol stress, which is known to be an efficient activator of the σ^B regulon. Figure 5 shows that both deletions were able to affect bacterial resistance to EtOH stress for exposure times of 90 min or longer. The nonpolar deletion of *yfkJ* led to a moderate reduction (around 50%) of EtOH stress resistance (Fig. 5). An identical phenotype was shown by the *B. subtilis* strain LM02, carrying a polar deletion of *yfkJ*, in two independent experiments (data not shown). The deletion of *ywlE* led to a more marked (more than 75%) decrease of *B. subtilis* survival (Fig. 5) after EtOH stress. The strain LM50 carrying a deletion of both phosphatases showed a phenotype similar to that of the Δ*ywlE* strain (Fig. 5).

DISCUSSION

In this study we cloned and biochemically characterized two LMPTPs (YfkJ and YwlE) from *B. subtilis*. The presence of two enzymatically active LMPTPs has been reported for several other bacteria, including *E. coli* (54) and *S. aureus* (48). The two enzymes were active on *p*NPP and tyrosine phosphosubstrates in vitro but showed significant differences in their biochemical properties. The optimal pH in the acidic range and the pattern of enzyme sensitivity to mutations of critical residues suggested that both enzymes dephosphorylate their substrate with a mechanism similar to that of known Cys-based PTPs. Overall the pattern of sensitivity of YfkJ and YwlE to inhibitors is very similar to that reported for eukaryotic and prokaryotic LMPTPs and in general for Cys-based PTPs. The insensitivity of YfkJ to vanadate represents an important ex-

ception and, to the best of our knowledge, has not been reported for any other LMPTP. Also the inhibition of YwlE by millimolar concentrations of NaPP that we observe has not been reported for other LMPTPs and might be of physiological relevance, as *B. subtilis* is known to contain between 1.2 and 6 mM pyrophosphate, depending on the growth conditions (31).

The kinetic parameters of YfkJ and YwlE against *p*NPP were similar to those of their orthologs in *S. aureus*, PtpA and PtpB, which are the only other LMPTPs characterized so far from gram-positive bacteria (48). YwlE showed good specific activity against tyrosine-phosphorylated substrates. In contrast, YfkJ was able to dephosphorylate only free *O*-phosphotyrosine. This suggests that YfkJ may have a stricter requirement for specific sequence determinants surrounding the phosphorylated residue. None of the two enzymes showed significant activity against other O- or N-phosphorylated amino acids.

The present study also showed that there are significant differences in chromosomal and operon structures between LMPTPs in gram-negative organisms and in *B. subtilis*, and between the two LMPTPs in *B. subtilis*. Gram-negative LMPTPs are usually located near a gene encoding a tyrosine kinase within *cps* or *cps*-like operons (55). No such gene could be identified in the operons containing YfkJ or YwlE, or even in their vicinity, in *B. subtilis*. Although no exhaustive biochemical comparison between LMPTP pairs isolated from gram-negative organisms has been reported to date, differences in biochemical behavior and chromosomal organization seem to be more common among gram-positive than gram-negative LMPTP pairs. Indeed, YfkJ and YwlE share much less similarity in primary structure to each other than LMPTP pairs encoded by gram-negative genomes, like the *E. coli* YccY (also called Etp) and Wzb (27, 55). Our phylogenetic analysis showed that LMPTP pairs in gram-positive organisms are evolutionarily distant from each other compared to their gram-negative counterparts. The genome context analysis for the two *B. subtilis* enzymes did not deliver specific predictions but provided useful guidelines for further experimental studies of functional coupling of each phosphatase gene with coclustered neighbors. It is tempting to speculate that each LMPTP might be involved in the control of the phosphorylation state of one or more of these proteins or their interaction partners.

Transcriptional analyses showed interesting differences between the two *B. subtilis* LMPTPs. The *yfkJ* promoter region contains a σ^B recognition sequence, and *yfkJ* transcription has
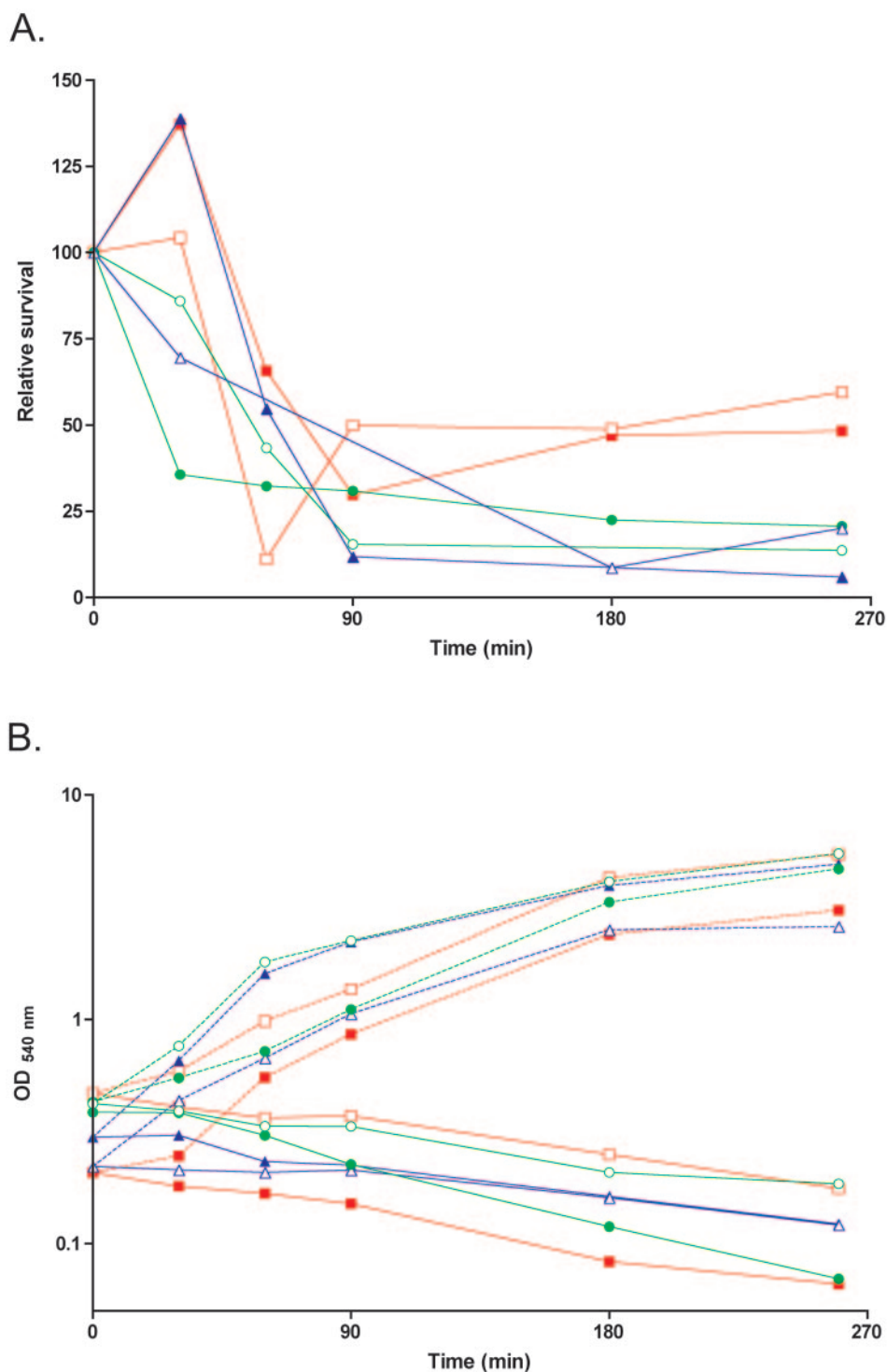
A.

B.

FIG. 5. Resistance of LM58 (ΔyfkJ), LM24 (ΔywlE), and LM50 (double deletion) *B. subtilis* strains to ethanol stress. Bacteria were grown in LB medium, and lethal stress was administered by the addition of 9% ethanol to early-log-phase cultures as described by Völker et al. (56). Appropriate dilutions of samples taken at the indicated time points were plated in duplicate on LB solid medium. Survival was calculated as the ratio of the average number of colonies at the indicated times after application of 9% ethanol stress to the number of colonies at time zero. Relative survival was calculated as a ratio between the survival of each strain and the survival of the wild-type JH642 strain under the same experimental conditions. (A) Relative survival after subjection to 9% ethanol stress of the ΔyfkJ (red lines), ΔywlE (blue lines), or double-deletion (green lines) strain. Results for the ΔyfkJ strain have been obtained by growing both the wild type and deletion strains in the presence of 1 mM IPTG. (B) Growth curves of bacteria used in the same experiments and of control bacteria not subjected to EtOH stress. In panels A and B, two independent experiments for each deletion strain (indicated by filled and empty symbols) are shown.

been shown by Price et al. (43) and by our data (Fig. 4) to be upregulated in a σ^B-dependent manner during ethanol stress. The 5′ region of the *ywlE* gene also showed promoter activity, which drove transcription of a reporter gene in a growth-dependent, but ethanol insensitive, pattern.

The stress-dependent upregulation of *yfkJ* transcription, together with the recent finding that *E. coli* Etp plays a critical role in bacterial resistance to heat stress (27), prompted us to analyze the possible role of YfkJ and YwlE in the ethanol stress resistance of *B. subtilis*. Genomic deletion of each phosphatase led to a phenotype of reduced bacterial resistance to ethanol stress, which was more pronounced in the *ywlE* deletion strain. Deletion of both phosphatases did not lead to an additive phenotype, suggesting that YwlE is at least partially able to compensate for the loss of YfkJ. The role of each phosphatase and their partial overlap in *B. subtilis* resistance to ethanol and possibly other stresses needs to be further investigated by complementation and cross-complementation experiments.

In gram-negative organisms tyrosine phosphorylation phenomena are known to be involved in the virulence of *Aeromonas* spp. (51), and interestingly, the expression of the tyrosine autokinase Etk was found to be restricted to some pathogenic strains of *E. coli* (22). A possible involvement of LMPTP genes in virulence would not be surprising, considering that stress resistance plays a role in the virulence of several pathogenic bacilli. For example *B. anthracis* needs to overcome the extreme oxidative stress and very low pH in the macrophage phagosome during outgrowth (16). The role of tyrosine phosphorylation pathways in the σ^B-dependent and -independent stress resistance of virulent bacilli also warrants further investigation.

In conclusion, we isolated two *B. subtilis* LMPTPs and found that they behave as bona fide tyrosine phosphatases. We also found that they play a role in ethanol stress resistance. Protein tyrosine phosphorylation has recently been shown to be present in *B. subtilis*. The first PTK and PTP pair with their substrate have recently been isolated from this organism and characterized (32). The final elucidation of the mechanism of action of YfkJ and YwlE in *B. subtilis* stress resistance will require the isolation of their physiological substrate(s) and/or interactor(s) during bacterial stress.

ACKNOWLEDGMENTS

REFERENCES

1. **Alonso, A., J. Sasin, N. Bottini, I. Friedberg, I. Friedberg, A. Osterman, A. Godzik, T. Hunter, J. Dixon, and T. Mustelin.** 2004. The set of genes encoding protein tyrosine phosphatase family members in the human genome. Cell **117:**699–711.
2. **Anagnostopoulos, C., and J. Spizizen.** 1961. Requirements for transformation in *Bacillus subtilis*. J. Bacteriol. **81:**741–746.
3. **Bender, M. H., and J. Yother.** 2001. CpsB is a modulator of capsule-associated tyrosine kinase activity in *Streptococcus pneumoniae*. J. Biol. Chem. **276:**47966–47974.
4. **Bennett, M. S., Z. Guan, M. Laurberg, and X. D. Su.** 2001. *Bacillus subtilis* arsenate reductase is structurally and functionally similar to low molecular weight protein tyrosine phosphatases. Proc. Natl. Acad. Sci. USA **98:**13577–13582.
5. **Bugert, P., and K. Geider.** 1997. Characterization of the *amsI* gene product as a low molecular weight acid phosphatase controlling exopolysaccharide synthesis of *Erwinia amylovora*. FEBS Lett. **400:**252–256.
6. **Callahan, C., D. Neri-Cortes, and M. P. Deutscher.** 2000. Purification and characterization of the tRNA-processing enzyme RNase BN. J. Biol. Chem. **275:**1030–1034.
7. **Chow, K., D. Ng, R. Stokes, and P. Johnson.** 1994. Protein tyrosine phosphorylation in *Mycobacterium tuberculosis*. FEMS Microbiol. Lett. **124:**203–207.
8. **Cirri, P., T. Fiaschi, P. Chiarugi, G. Camici, G. Manao, G. Raugei, and G. Ramponi.** 1996. The molecular basis of the differing kinetic behavior of the two low molecular mass phosphotyrosine protein phosphatase isoforms. J. Biol. Chem. **271:**2604–2607.
9. **Dadssi, M., and A. J. Cozzone.** 1990. Evidence of protein-tyrosine kinase activity in the bacterium *Acinetobacter calcoaceticus*. J. Biol. Chem. **265:**20996–20999.
10. **DeVinney, I., I. Steele-Mortimer, and B. B. Finlay.** 2000. Phosphatases and kinases delivered to the host cell by bacterial pathogens. Trends Microbiol. **8:**29–33.
11. **Dowds, B. C., and J. A. Hoch.** 1991. Regulation of the oxidative stress response by the *hpr* gene in *Bacillus subtilis*. J. Gen. Microbiol. **137:**1121–1125.
12. **Ferrari, E., D. J. Henner, M. Perego, and J. A. Hoch.** 1988. Transcription of *Bacillus subtilis* subtilisin and expression of subtilisin in sporulation mutants. J. Bacteriol. **170:**289–295.
13. **Foster, R., J. Thorner, and G. S. Martin.** 1989. Nucleotidylation, not phosphorylation, is the major source of the phosphotyrosine detected in enteric bacteria. J. Bacteriol. **171:**272–279.
14. **Fouet, A., O. Namy, and G. Lambert.** 2000. Characterization of the operon encoding the alternative σ^B factor from *Bacillus anthracis* and its role in virulence. J. Bacteriol. **182:**5036–5045.
15. **Grangeasse, C., P. Doublet, C. Vincent, E. Vaganay, M. Riberty, B. Duclos, and A. J. Cozzone.** 1998. Functional characterization of the low-molecular-mass phosphotyrosine-protein phosphatase of *Acinetobacter johnsonii*. J. Mol. Biol. **278:**339–347.
16. **Guidi-Rontani, C.** 2002. The alveolar macrophage: the Trojan horse of *Bacillus anthracis*. Trends Microbiol. **10:**405–409.
17. **Harwood, C. R., and S. M. Cutting (ed.).** 1990. Molecular biological methods for *Bacillus*. John Wiley and Sons, New York, N.Y.
18. **Heurgue-Hamard, V., S. Champ, A. Engstrom, M. Ehrenberg, and R. H. Buckingham.** 2002. The *hemK* gene in *Escherichia coli* encodes the N^5-glutamine methyltransferase that modifies peptide release factors. EMBO J. **21:**769–778.
19. **Himanen, J. P., and D. B. Nikolov.** 2003. Eph receptors and ephrins. Int. J. Biochem. Cell. Biol. **35:**130–134.
20. **Howell, L. D., C. Griffiths, L. W. Slade, M. Potts, and P. J. Kennelly.** 1996. Substrate specificity of IphP, a cyanobacterial dual-specificity protein phosphatase with MAP kinase phosphatase activity. Biochemistry **35:**7566–7572.
21. **Hunter, T.** 1998. The role of tyrosine phosphorylation in cell growth and disease. Harvey Lect. **94:**81–119.
22. **Ilan, O., Y. Bloch, G. Frankel, H. Ullrich, K. Geider, and I. Rosenshine.** 1999. Protein tyrosine kinases in bacterial pathogens are associated with virulence and production of exopolysaccharide. EMBO J. **18:**3241–3248.
23. **Kelly-Wintenberg, K., T. Anderson, and T. C. Montie.** 1990. Phosphorylated tyrosine in the flagellum filament protein of *Pseudomonas aeruginosa*. J. Bacteriol. **172:**5135–5139.
24. **Kennelly, P. J.** 2002. Protein kinases and protein phosphatases in prokaryotes: a genomic perspective. FEMS Microbiol. Lett. **206:**1–8.
25. **Kennelly, P. J.** 2003. Archaeal protein kinases and protein phosphatases—insights from genomics and biochemistry. Biochem. J. **370:**373–389.
26. **Kholod, N., and T. Mustelin.** 2001. Novel tools for studying protein complexes: vectors for co-expression of two proteins in *Escherichia coli*. BioTechniques **31:**322–328.
27. **Klein, G., C. Dartigalongue, and S. Raina.** 2003. Phosphorylation-mediated regulation of heat shock response in *Escherichia coli*. Mol. Microbiol. **48:**269–285.
28. **Kristich, C. J., G. D. Glekas, and G. W. Ordal.** 2003. The conserved cytoplasmic module of the transmembrane chemoreceptor McpC mediates carbohydrate chemotaxis in *Bacillus subtilis*. Mol. Microbiol. **47:**1353–1366.
29. **Kunst, F., et al.** 1997. The complete genome sequence of the Gram-positive bacterium *Bacillus subtilis*. Nature **390:**249–256.
30. **Mijakovic, I., L. Musumeci, L. Tautz, D. Petranovic, R. Edwards, P. R. Jensen, T. Mustelin, J. Deutscher, and N. Bottini.** 2005. In vitro characterization of *B. subtilis* protein tyrosine phosphatase YwqE. J. Bacteriol. **187:**3384–3390.
31. **Mijakovic, I., S. Poncet, A. Galinier, V. Monedero, S. Fieulaine, J. Janin, S. Nessler, J. A. Marquez, K. Scheffzek, S. Hasenbein, W. Hengstenberg, and J. Deutscher.** 2002. Pyrophosphate-producing protein dephosphorylation by HPr kinase/phosphorylase: a relic of early life? Proc. Natl. Acad. Sci. USA **99:**13442–13447.
32. **Mijakovic, I., S. Poncet, G. Boel, A. Maze, S. Gillet, E. Jamet, P. Decottignies, C. Grangeasse, P. Doublet, P. Le Marechal, and J. Deutscher.** 2003.

Transmembrane modulator-dependent bacterial tyrosine kinase activates UDP-glucose dehydrogenases. EMBO J. **22:**4709–4718.

33. **Miller, J. H.** 1972. Experiments in molecular genetics, p. 352–355. Cold Spring Harbor Laboratory, Cold Spring Harbor, N.Y.

34. **Morona, J. K., J. C. Paton, D. C. Miller, and R. Morona.** 2000. Tyrosine phosphorylation of CpsD negatively regulates capsular polysaccharide biosynthesis in *Streptococcus pneumoniae.* Mol. Microbiol. **35:**1431–1442.

35. **Morona, J. K., R. Morona, D. C. Miller, and J. C. Paton.** 2002. *Streptococcus pneumoniae* capsule biosynthesis protein CpsB is a novel manganese-dependent phosphotyrosine-protein phosphatase J. Bacteriol. **184:**577–583.

36. **Mustelin, T., G. S. Feng, N. Bottini, A. Alonso, N. Kholod, D. Birle, J. Merlo, and H. Huynh.** 2002. Protein tyrosine phosphatases. Front. Biosci. **7:**85–142.

37. **Na, J. G., I. Pinto, and M. Hampsey.** 1992. Isolation and characterization of *SUA5,* a novel gene required for normal growth in *Saccharomyces cerevisiae.* Genetics **131:**791–801.

38. **Osterman, A., and R. Overbeek.** 2003. Missing genes in metabolic pathways: a comparative genomics approach. Curr. Opin. Chem. Biol. **7:**1–14.

39. **Ostrovsky, P. C., and S. Maloy.** 1995. Protein phosphorylation on serine, threonine, and tyrosine residues modulates membrane-protein interactions and transcriptional regulation in *Salmonella typhimurium.* Genes Dev. **9:**2034–2041.

40. **Perego, M.** 1993. Integrational vectors for genetic manipulation in *Bacillus subtilis,* p. 615–624. *In* A. L. Sonenshein, J. A. Hoch, and R. Losick (ed.), *Bacillus subtilis* and other gram-positive bacteria: biochemistry, physiology, and molecular genetics. American Society for Microbiology, Washington, D.C.

41. **Potts, M., H. Sun, K. Mockaitis, P. J. Kennelly, D. Reed, and N. K. Tonks.** 1993. A protein-tyrosine/serine phosphatase encoded by the genome of the cyanobacterium *Nostoc commune* UTEX 584. J. Biol. Chem. **268:**7632–7635.

42. **Preneta, R., S. Jarraud, C. Vincent, P. Doublet, B. Duclos, J. Etienne, and A. J. Cozzone.** 2002. Isolation and characterization of a protein-tyrosine kinase and a phosphotyrosine-protein phosphatase from *Klebsiella pneumoniae.* Comp. Biochem. Physiol. B **131:**103–112.

43. **Price, C. W., P. Fawcett, H. Ceremonie, N. Su, C. K. Murphy, and P. Youngman.** 2001. Genome-wide analysis of the general stress response in *Bacillus subtilis.* Mol. Microbiol. **41:**757–774.

44. **Ramponi, G., and M. Stefani.** 1997. Structural, catalytic, and functional properties of low M_r phosphotyrosine protein phosphatases. Evidence of a long evolutionary history. Int. J. Biochem. Cell. Biol. **29:**279–292.

45. **Rayapureddi, J. P., C. Kattamuri, B. D. Steinmetz, B. J. Frankfort, E. J. Ostrin, G. Mardon, and R. S. Hegde.** 2003. Eyes absent represents a class of protein tyrosine phosphatases. Nature **426:**295–298.

46. **Sau, S., N. Bhasin, E. R. Wann, J. C. Lee, T. J. Foster, and C. Y. Lee.** 1997. The *Staphylococcus aureus* allelic genetic loci for serotype 5 and 8 capsule expression contain the type-specific genes flanked by common genes. Microbiology **143:**2395–2405.

47. **Smith, S. C., P. J. Kennelly, and M. Potts.** 1997. Protein-tyrosine phosphorylation in the archaea. J. Bacteriol. **179:**2418–2420.

48. **Soulat, D., E. Vaganay, B. Duclos, A. L. Genestier, J. Etienne, and A. J. Cozzone.** 2002. *Staphylococcus aureus* contains two low-molecular-mass phosphotyrosine protein phosphatases. J. Bacteriol. **184:**5194–5199.

49. **Tatusov, R. L., E. V. Koonin, and D. J. Lipman.** 1997. A genomic perspective on protein families. Science **278:**631–637.

50. **Taylor, J. R.** 1997. An introduction to error analysis. University Science Books, Sausalito, Calif.

51. **Thomas, S. R., and T. J. Trust.** 1995. Tyrosine phosphorylation of the tetragonal paracrystalline array of *Aeromonas hydrophila*: molecular cloning and high-level expression of the S-layer protein gene. J. Mol. Biol. **245:**568–581.

52. **Tzeng, Y. L., and J. A. Hoch.** 1997. Molecular recognition in signal transduction: the interaction surfaces of the Spo0F response regulator with its cognate phosphorelay proteins revealed by alanine scanning mutagenesis J. Mol. Biol. **272:**200–212.

53. **Tzeng, Y. L., X. Z. Zhou, and J. A. Hoch.** 1998. Phosphorylation of the Spo0B response regulator phosphotransferase initiating development in *Bacillus subtilis.* J. Biol. Chem. **273:**23849–23855.

54. **Vincent, C., P. Doublet, C. Grangeasse, E. Vaganay, A. J. Cozzone, and B. Duclos.** 1999. Cells of *Escherichia coli* contain a protein-tyrosine kinase, Wzc, and a phosphotyrosine-protein phosphatase, Wzb. J. Bacteriol. **181:**3472–3477.

55. **Vincent, C., B. Duclos, C. Grangeasse, E. Vaganay, M. Riberty, A. J. Cozzone, and P. Doublet.** 2000. Relationship between exopolysaccharide production and protein-tyrosine phosphorylation in Gram-negative bacteria. J. Mol. Biol. **304:**311–321.

56. **Völker, U., B. Maul, and M. Hecker.** 1999. Expression of the sigmaB-dependent general stress regulon confers multiple stress resistance in *Bacillus subtilis.* J. Bacteriol. **181:**3942–3948.

57. **Wo, Y. Y., A. L. McCormack, J. Shabanowitz, D. F. Hunt, J. P. Davis, G. L. Mitchell, and R. L. Van Etten.** 1992. Sequencing, cloning, and expression of human red cell-type acid phosphatase, a cytoplasmic phosphotyrosyl protein phosphatase. J. Biol. Chem. **267:**10856–10865.

58. **Zhang, M., C. V. Stauffacher, D. Lin, and R. L. Van Etten.** 1998. Crystal structure of a human low molecular weight phosphotyrosyl phosphatase. Implications for substrate specificity. J. Biol. Chem. **273:**21714–21720.

59. **Zimmer, M. A., H. Szurmant, M. M. Saulmon, M. A. Collins, J. S. Bent, and G. W. Ordal.** 2002. The role of heterologous receptor in McpB-mediated signaling in *Bacillus subtilis* chemotaxis. Mol. Microbiol. **45:**555–568.